Journal of Archaeological Science 36 (2009) 2481–2492

Contents lists available at ScienceDirect

Journal of Archaeological Science

journal homepage: http://www.elsevier.com/locate/jas

Review

Assessment of material characteristics of ancient concretes, Grande Aula, Markets of Trajan, Rome

Marie D. Jackson[a,*], John M. Logan[b,1], Barry E. Scheetz[c,2], Daniel M. Deocampo[d,3], Carl G. Cawood[e,4], Fabrizio Marra[f,5], Massimo Vitti[g,6], Lucrezia Ungaro[h,7]

[a] Department of History, PO Box 6023, Northern Arizona University, Flagstaff, AZ 86011-6023, USA
[b] Department of Geological Sciences, University of Oregon, Eugene, OR 97403, USA
[c] Center for Dirt and Gravel Studies, North American Refractories Building, Room 151, The Pennsylvania State University, 3127 Research Drive, State College, PA 16801, USA
[d] Department of Geosciences, PO Box 4105, Georgia State University, Atlanta, GA 30302, USA
[e] Department of Civil and Environmental Engineering, PO Box 15600, Northern Arizona University, Flagstaff, AZ 86011-15600, USA
[f] Istituto Nazionale di Geofisica e Vulcanologia, Via di Vigna Murata 605, Rome 00143, Italy
[g] Sovraintendenza per i Beni Culturali del Comune di Roma, Ufficio Fori Imperiali, Via Quattro Novembre 94, Rome 00187, Italy
[h] Sovraintendenza ai Beni Culturali, Servizio V, Museo dei Fori Imperiali, Museo della Civiltà Romana, Coordinamento Progetti Multimediali, Servizio Civile, Progetti Europei, Via Quattro Novembre 94, Rome 00187, Italy

ARTICLE INFO

Article history:
Received 8 March 2009
Received in revised form
8 July 2009
Accepted 9 July 2009

Keywords:
Ancient Rome
Concrete
Pozzolanic mortar
Strätlingite
Tensile strength
Point load tests

ABSTRACT

The Grande Aula, or Great Hall, of the Markets of Trajan (AD 96 to 115) is an intact example of the domed, concrete architecture of imperial Rome. Petrographic, x-ray diffraction, chemical, and SEM analyses demonstrate that wall mortars contain Pozzolane Rosse volcanic ash aggregate (*harenae fossiciae*) and strätlingite, a complex calcium aluminate cement hydrate (C_2 ASH_8) that gives modern cements good durability and compressive strength. Specific gravity tests and a new petrographic method for assessing bulk densities indicate unit weights of about 1750 kg/m^3 for the wall mortars and 1430–1640 kg/m^3 for the pumice bearing, vaulted ceiling mortars. Innovative point load source tests record the tensile strengths ($\mathbf{f}_t$) of the aggregate and interfacial elements of the conglomeratic concrete fabric. These suggest $\mathbf{f}_t$ of about 2.7 MPa for brick, 1.2 MPa for Tufo Lionato tuff, and 0.9 MPa for Tufo Giallo della Via Tiberina tuff coarse aggregate (*caementa*), based on a tentative, approximate correlation with splitting (Brazilian) tests. The pozzolanic mortar and interfacial zones have lower $\mathbf{f}_t$ in the range of 0.8 MPa to 0.5 MPa. The relatively low mortar strength and its somewhat tenuous adhesion to the coarse aggregate suggests that the *caementa* may have arrested the propagation of tensile microcracks that formed in the mortar, thereby increasing the composite tensile strength of the concrete. Roman builders selected the complex aggregate mixes to optimize the performance of the wall and vault concretes.

1. Introduction

The Grande Aula, or Great Hall, of the Markets of Trajan, is one of the most impressive, imperial era monuments in Rome (Vitti, 2007). Constructed from 96 to 115 AD under the direction of Apollodorus of Damascus, the architect who was directly charged by Emperor Trajan to carry out the construction of the Forum of Trajan, the Grande Aula presents numerous significant architectural innovations (Giovannoni, 1913; Bianchini, 1991; Lancaster, 2000; Vitti, 2007). It consists of a large rectangular room, 36 m long and 8.5 m wide, that is spanned by a concrete vaulted ceiling composed of six consecutive cross vaults, supported by slender lateral arches, thick concrete walls, and travertine cut-stone masonry (Fig. 1). The walls have triangular brick facings that enclose a concrete core, or nucleus, composed of various types of coarse aggregate bound together by well-preserved pozzolanic mortars (Fig. 2). The mortars contain *harenae fossiciae*, the excavated sand aggregate described by Vitruvius (*On Architecture* 2.4.1–3), which is mainly dark gray

* Corresponding author. Northern Arizona University, Department of History, Building 18 Room 219, Flagstaff, AZ 86011-6023, USA. Tel.: +1 928 774 5959.
E-mail address: Marie.Jackson@nau.edu (M.D. Jackson).
1 Tel.: +1 541 347 7403; fax: +1 541 347 9268. JMLLOGAN@aol.com.
2 Tel.: +1 404 413 5759; fax: +1 404 413 5768. deocampo@gsu.edu.
3 Tel.: +1 814 863 5616; fax: +1 814 865 9668. se6@psu.edu.
4 Tel.: +1 928 526 0998. carlcawood@aol.com.
5 Tel.: +39 06 5186 0420. marra@ingv.it.
6 Tel.: +39 06 6978 0532. massimo.vitti@comune.roma.it.
7 Tel.: +39 06 6994 1020. lucrezia.ungaro@comune.roma.it.

0305-4403/$ – see front matter
doi:10.1016/j.jas.2009.07.011

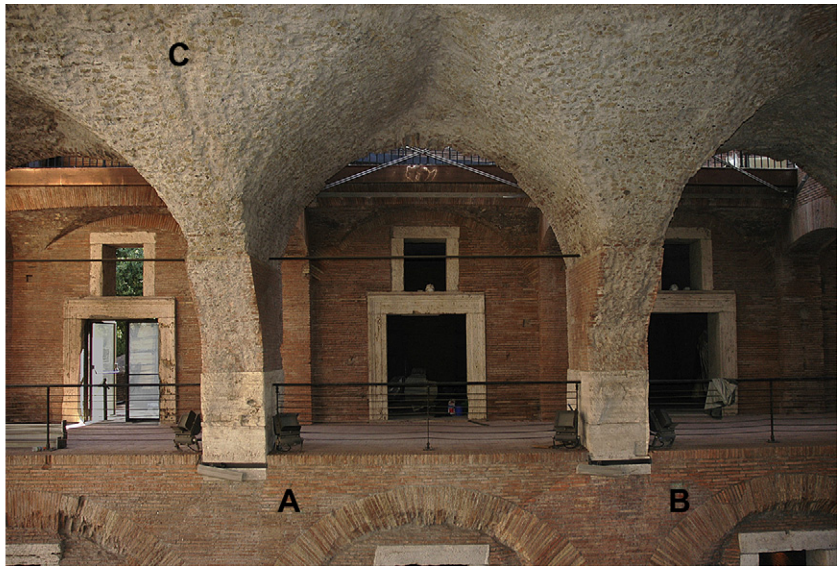

Fig. 1. Locations of samples, Grande Aula, Markets of Trajan. Conglomeratic concrete of the nucleus of the eastern wall, 19 cm diameter, hollow, thin walled drill cores: A) core 8, Bay 135; core 20, Bay 136. C) Pozzolanic mortar of the vaulted ceiling, Bay 134/135.

and dusky red Pozzolane Rosse volcanic ash (Jackson et al., 2007). In contrast, the cross-vaulted ceiling has no brick facing and its mortar contains Pozzolane Rosse ash as well as light gray pumices.

Compressive strength tests of ancient concretes and bricks, and reproductions of Roman pozzolanic mortars and concrete walls suggest that imperial era wall concretes have uniaxial compressive strengths ($\mathbf{f}_c$) of about 6 MPa (Table 1). The compositions, proportions, and installation techniques of coarse aggregate components, or *caementa*, are defining factors in determining the overall mechanical strength of the ancient concretes (Table 1) (Samuelli Ferretti, 1997; Giavarini et al., 2006). Indeed, Vitruvius describes the role of the *caementicium*, or unhewn quarry stone, in the durability of first century BC concrete walling (*On Architecture*, 2.8.1–7; Granger, 1931). Little information exists, however, about the processes of fracture and failure in the ancient conglomeratic concretes. Cracks may nucleate in the pozzolanic mortar, in fragments of volcanic tuff or brick coarse aggregate, or at interfacial adhesive zones at the contacts of the various volcanic tuff or brick *caementa* with the pozzolanic mortar. These data are central to constructing accurate numerical models to evaluate the stability of the imperial age Roman monuments (e.g. Croci, 1993; Samuelli Ferretti, 2005; Brune and Perucchio, in press; Perucchio and Brune,

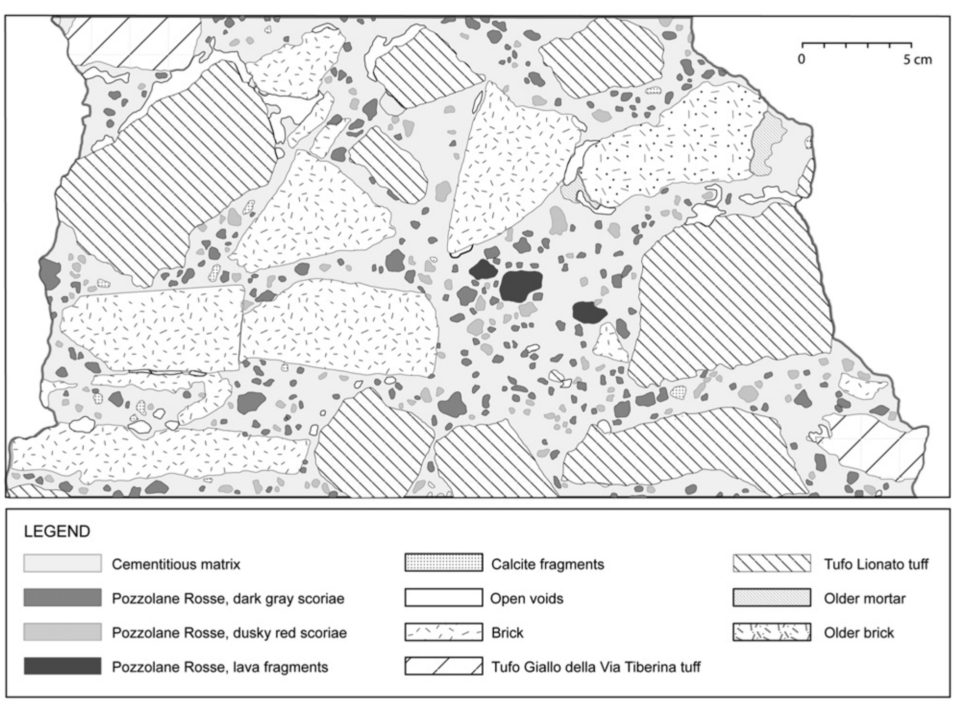

Fig. 2. Compositional map of part of the perimeter surface of concrete core 20. The light gray area represents the cementitious matrix, composed of pozzolanic cements and Pozzolane Rosse volcanic ash less than 2 mm in diameter.

Table 1
Summary of current experimental data for the material and physical properties of the raw volcanic aggregates of the Grande Aula concretes, ancient Roman pozzolanic mortars and concretes, and Roman volcanic tuff and travertine dimension stone masonry.

Type of Building Material		G	Unit Weight	Ab	f_c	f_t	E
		Bulk specific gravity	(Averages) kg/m^3	wt % water sorption	Compressive strength, MPa	Tensile strength, MPa	Elastic Modulus
Fine Aggregate *(harenae fossiciae)*							
Pozzolane Rosse	Altered scoriae, intermediate and least altered facies	1.6–1.8	1600–1800	18–22	*in situ* tests[a] 0.15-0.25 MPa	*in situ* tests[a] 0.09 MPa	/
Pozzolane Rosse	Lava lithic fragments, similar to Vallerano lava flow						
	Vallerano lava [b]	2.81–2.83	2820	0.73	280	19	478,000
Mortar pumice,[c] Colosseum	White, sanidine-bearing pumice	/	600–700	/	/	/	/
Rhyolitic pumice[d]	Light grey, sand- to gravel-sized, glassy pumice	0.84–0.87	840–870	18–22	/	1.1–2.1	2400
Bay of Naples[e] pyroclastics	Flegrean pumice and lapilli tuffs	9.9-13.7	990-1370	30	2.96	/	2760
Coarse Aggregate *(caementa)*							
Tufo Giallo della Via Tiberina	Compact vitric-crystal tuff [f]	1.52	1520	20	15	/	3154
	Pumiceous tuff[g]	1.27	1270	24	6.5	0.78	/
Tufo Lionato	Vitric-crystal-lithic tuff,[f] Salone quarry	1.73	1679	15	17	/	3967
	Range of localities[h]	/	1250–1850	19–41	3.7–16.6	0.82 – 1.60	/
Ancient Brick [i]	Small parallelepipeds	/	1603	/	17	3.33	13,400
Pozzolanic Mortars and Concretes							
Ancient concretes from monuments [i]	Various formulations	/	13.5–17.7	/	0.98–6.7	0.8–0.9	1750–9170
Experimental mortar[i]	Lime and Pozzolane Rosse	/	/	/	11.7–12.3	0.95–1.09	3160
Experimental concrete panels[i]	Brick and tuff aggregates	/	/	/	6.2	/	2560
Dimension Stone							
Lapis Albanus[f]	Lithic-crystal tuff	1.87	2018	11	19	/	3734
Travertine[f]	Tivoli quarries	2.58	2580	0.6	105	11–14[j]	48,870–62,600[j]
Carrarra Marble[k]	Various quarries	2.7	2700	0.29	130	4.8	68,500

[a] Ventriglia, 1971, *La Geologia della città di Roma.* (in situ Pozzolane Rosse deposit).
[b] Penta, 1956, *I Materiali Naturali da Costruzione del Lazio*.
[c] Lancaster, 2005, *Concrete Vaulted Construction in Imperial Rome*.
[d] Lightweight California Pumice; http://www.clppumice.com/engineering.html.
[e] http://www.nato.int/shape/community/budfin/ifib/aco-nap-61/relazione%20geotecnica%20-lagopatria-italiano.doc.
[f] Jackson et al., 2005, *Archaeometry*.
[g] Nappi et al., 1979, *Bolletino Societa Geologica Italiano*.
[h] De Casa et al., 1999, *Geologia Romana*.
[i] Samuelli Ferretti, 1997, *Materiali e Strutture* and Giavarini et al., 2006, *Fracture and Failure of Natural Building Stones*.
[j] Industrial sources, Tivoli and Guidonia.
[k] Logan, 2006, *Fracture and Failure of Natural Building Stones*.

in press). The results of compressive strength studies of maritime-type Roman concretes with pumiceous aggregate from the Bay of Naples (Oleson et al., 2006; Goldsworthy and Min, 2009) are not directly applicable to the wall concretes, because the compositions and textures of the pozzolanic mortars are quite different, as noted by Vitruvius (*On Architecture* 2.6.1–6; 2.4.1–2) (Jackson et al., 2007; Vola and Gotti, in press).

The purpose of this paper is to assess the material characteristics of the concrete wall nuclei of the Grande Aula, derived from cores drilled from Bays 135 and 136 (Fig. 1). We introduce new methods for describing the compositions of Roman concretes, first situating the coarse aggregates within the geologic bedrock of Rome, and then using petrographic and geochemical investigations to identify the textures and compositions of pozzolanic cements, and the unit weights of the mortars and concretes. From point source load tests (ISRM, 1985) we identify patterns of fracture within the wall concrete, and its anisotropic properties and resistance to tensile stresses. Finally, we integrate these data to assess the durability of the concretes, evaluate Roman expertise in designing the concrete masonry, and provide archaeologists with new techniques for determining the material characteristics of diverse Roman conglomeratic concretes.

2. Compositions of the wall core concretes

Compositional maps made by tracing the boundaries of all aggregate components greater than 2 mm in diameter on plastic sheets wrapped around the perimeter surfaces of two 19 cm diameter cylinders, 22 cm and 27 cm in length, drilled from the walls of Bay 135 and Bay 136 (Fig. 1), show representative areas of the conglomeratic wall nucleus concrete (Fig. 2). Similar compositional maps could be generated for other concrete structures by tracing aggregate constituents on plastic sheets lain on flat masonry surfaces.

The very light gray areas of the compositional map represent the cementitious matrix of the pozzolanic mortar. This is the fundamental binding substance of the concrete, composed stable, enduring, alkali- and alumina- rich cement hydrates (Langton and Roy, 1984), and mainly Pozzolane Rosse volcanic ash aggregate with altered scoriae less than 2 mm in diameter. The ash contains altered scoriae, crystal fragments (mainly leucite, clinopyroxene, and occasional biotite), lava rock fragments, and the unreacted traces of natural argillic and zeolitic alteration components from an intermediate alteration facies with reddened scoriae and a least altered facies with dark gray scoriae (Jackson et al., in press).

The *caementa* of the conglomeratic wall concrete have diverse material characteristics (Table 1). Tufo Lionato is a compact, light brown (5YR 4/4 to 5YR 5/6 Munsell Color), moderately durable tuff erupted from the Alban Hills volcanic district south east of Rome, with oven-dry uniaxial compressive strength ($\mathbf{f_c}$) of about 17 MPa (Jackson et al., 2005; see Jackson and Marra, 2006 for geologic maps). Yellowish brown (10YR 6/2 Munsell Color), Tufo Giallo della Via Tiberina is a porous, weakly durable tuff from the Monti Sabatini volcanic district north of Rome. Pumiceous varieties, which resemble the *caementa* of the wall nucleus, have ambient $\mathbf{f_c}$ in the range of 6.5 MPa, and tensile strengths of about 1/10 to 1/6 $\mathbf{f_c}$ (Nappi et al., 1979). In comparison, Roman brick *caementa* have ambient $\mathbf{f_c}$ of about 17 MPa, and tensile strength of about 3 MPa (Samuelli Ferretti, 1997). The wide dispersion of the brick test results, coupled with a rapid decline in load carrying capacity after the peak load point, indicates that the brick may display fragile, inconsistent fracture behavior in Roman concretes (Samuelli Ferretti, 1997). The tuffs also display brittle, linear elastic behavior at low stress levels in compressive strength tests (Nappi et al., 1979; De Casa et al., 1999), especially under conditions of high relative humidity (Jackson et al., 2005).

Despite the brittle characteristics of the coarse aggregate, the wall concrete is exceptionally coherent and well cemented. Builders evidently compacted the wet concrete mass quite forcefully, vigorously pressing the mortar against the *caementa* and into its voids. In general, the contacts between the *caementa* and mortar are well defined and tightly bonded. However, intermittent open voids may occur along mortar-*caementa* contacts, which produce gaps in the monolithic bond between the mortar and coarse aggregate (Fig. 2).

3. Pozzolanic cements of the wall mortars

Petrographic point count analyses, with 500–600 sites per standard thin section, indicate that the mortars of the wall concretes (Table 2) contain relative abundances of about 40% Pozzolane Rosse volcanic ash, 2–3% ground Tufo Lionato tuff, 50% cementitious phases, and <5% open space. Vitruvius, in first century BC, and Pliny, in first century AD, gave recommendations for the ratio of lime that should be mixed with excavated sand (*harenae fossiciae*) aggregate, about 1:3 or 1:4 (*On Architecture*, 2.5.1 (Granger, 1931); *Natural History*, 36.175–177 (Eichholz, 1962). The nearly equal abundances of pozzolanic aggregate and cementitious products (Table 2) suggest that either the builders did not use these

Table 2
Material characteristics of pozzolanic mortars and concretes from the Grande Aula and Markets of Trajan. Mortar constituents were determined through petrographic point counts of thin sections. Water sorption and unit weight were determined through ASTM C-97-96 tests and petrographic analyses.

	Sample	Coarse Aggregate	Mortar Constituents	Water Sorption	Unit Weight
		caementa	*harenae fossiciae*	weight %	kg/m^3
			percent by volume, based on point counts	**Ab**	
Mortars					
EAST WALL, GRANDE AULA, BAY135	GRAULA20a-C1	mainly brick fragments, Tufo Lionato tuff, Tufo Giallo della Via Tiberina tuff	Pozzolane Rosse, mainly dark gray (N3) least altered facies with less moderate red (5R 4/6) intermediate alteration facies, 43%; finely ground Tufo Lionato, 2-3%; pozzolanic cements and calcite, 51%; open space, 2-3%	26	1720
VAULT INTRADOS, GRANDE AULA, BAY 134/135	GRAULA-C2	mainly Tufo Giallo della Via Tiberina tuff	Pozzolane Rosse, mainly dark gray (N3) least altered facies, with a fine fraction of moderate red (5R 4/6) intermediate alteration facies, 19%; Tufo Giallo della Via Tiberina and Tufo Lionato 3-4%; pozzolanic cements and calcite 35%; light gray pumice and open space, 41%	31	∼1430[a]
VAULT INTRADOS, GRANDE AULA, BAY134/135	GRAULA-C3	mainly Tufo Giallo della Via Tiberina tuff	Pozzolane Rosse, mainly least altered facies,with a fine fraction of moderate red (5R 4/6) intermediate alteration facies, 12%; Tufo Giallo della Via Tiberina and Tufo Lionato 5%; pozzolanic cements and calcite 55%; light gray pumice and open space, 28%	/	∼1640[a]
WALL CORE, RADIAL PIER Bay 246	MERCTRAI-C1	mainly brick fragments	Pozzolane Rosse, mainly dark gray (N3) and dusky red least (5R 3/4) altered facies, 41%; finely ground Tufo Lionato, 3%; pozzolanic cements and calcite, 51%; open space, 5%	12	1785
Concretes					
WALL CORE, GRANDE AULA BAY136	CORE 8 A (1)	brick, Tufo Lionato tuff, Tufo Giallo della Via Tiberina tuff, a few recycled concrete fragments.	Pozzolane Rosse volcanic ash, ∼40–50%: mainly least altered facies scoriae, dark gray (N3); upper least altered facies scoriae, very dark red (5R 3/6); intermediate alteration facies scoriae, moderate red (5R 4/6); and lava rock fragments, dark gray (N3). Pozzolanic cements and calcite, ∼50%. Open space, 2–5%.Rare tuff, brick, and calcite fragments.	21	1495
	CORE 8 B (2)			17	1552
WALL CORE, GRANDE AULA BAY135	CORE 20 B (3)			24	1448
	CORE 20 A (4)			20	1481

[a] Computed from sums of unit weights of constituents determined by point counts of thin sections.

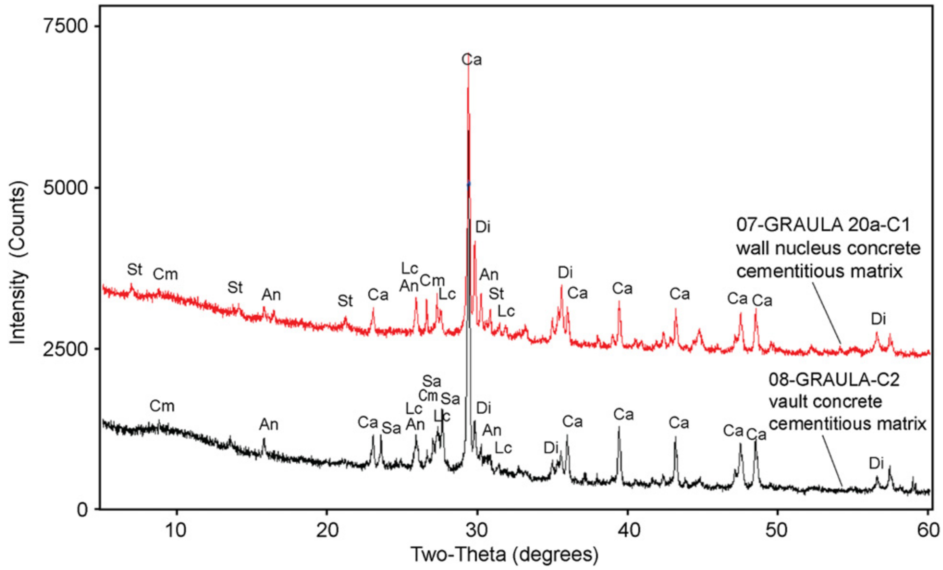

Fig. 3. X-ray diffraction analyses of pozzolanic mortars of the Grande Aula. b) cementitious matrix with Pozzolane Rosse mortar aggregate from the concrete wall nucleus, sample 07-GRAULA20a-C1; c) cementitious matrix with pumice and Pozzolane Rosse mortar aggregate from the concrete vaulted ceiling, sample 08-GRAULA-C2. Primary volcanic minerals: Sa: sanidine, Lc: leucite, Di: diopside (clinopyroxene); Secondary alteration minerals in ashes: An: analcime, Cm: clay mineral; Primary cement hydrate: St: strätlingite; Secondary alteration of cement hydrates: Ca: calcite.

proportions of raw materials in the original mortar mixture, and/or there is not a direct correspondence between these original proportions and the cured mortar constituents.

Pozzolane Rosse is a highly potassic, pyroclastic flow deposit (Trigila et al., 1995) that erupted about 456,000 years ago from the Alban Hills volcanic district (Karner et al., 2001; Marra et al., 2009). Petrographic studies of the mortars indicate that some altered Pozzolane Rosse scoriae preserve traces of opal and poorly crystalline clay, while others preserve traces of zeolites, both phillipsite and chabazite. These surface coatings are secondary, or authigenic, components of chemical weathering produced by a mid-Pleistocene soil that formed on the surface of the deposit (Karner and Marra, 1998; Jackson et al., in press). The altered ash generates good pozzolanic reactivity with Roman hydrated lime, which has very pure compositions with about 95 weight percent CaO and less than 0.3 weight percent Al_2O_3 (Sersale and Orsini, 1969; Jackson et al., 2007). Pozzolans are inorganic materials containing reactive constituents, generally aluminates and silicates, which combine with lime in the presence of moisture to form stable binding hydrates (Massazza, 1998). This is the "reactive capacity", or *potestas,* that Vitruvius describes for ideal *harenae fossiciae* (*On Architecture*,. 2.6.6)(Jackson et al., 2007, 41).

X-ray diffraction (XRD) analyses (Fig. 3) of the wall mortar specimen, 07-GRAULA20a-C1, shows leucite, clinopyroxene (diopside), and analcime associated with Pozzolane Rosse volcanic ash aggregate; strätlingite pozzolanic cements; and calcite, a secondary alteration component of cementitious binding phases. Traces of authigenic Pozzolane Rosse constituents (Jackson et al., in press) apparently occur in such tiny amounts that they do not produce sharp peaks. An amorphous component below 20° 2Θ may reflect amorphous pozzolanic cementitious gels. The peak recorded in the diffractogram of the wall mortar for strätlingite, a complex calcium aluminate cement hydrate ($2CaO\ Al_203\ SiO_2\ 8H_2O$ or $C_2\ ASH_8$), is of particular interest, as it has not been previously recognized in ancient concretes.

Strätlingite is one of the main strength-giving cementitious phases in modern calcium aluminate cements (Taylor, 2004: 304).

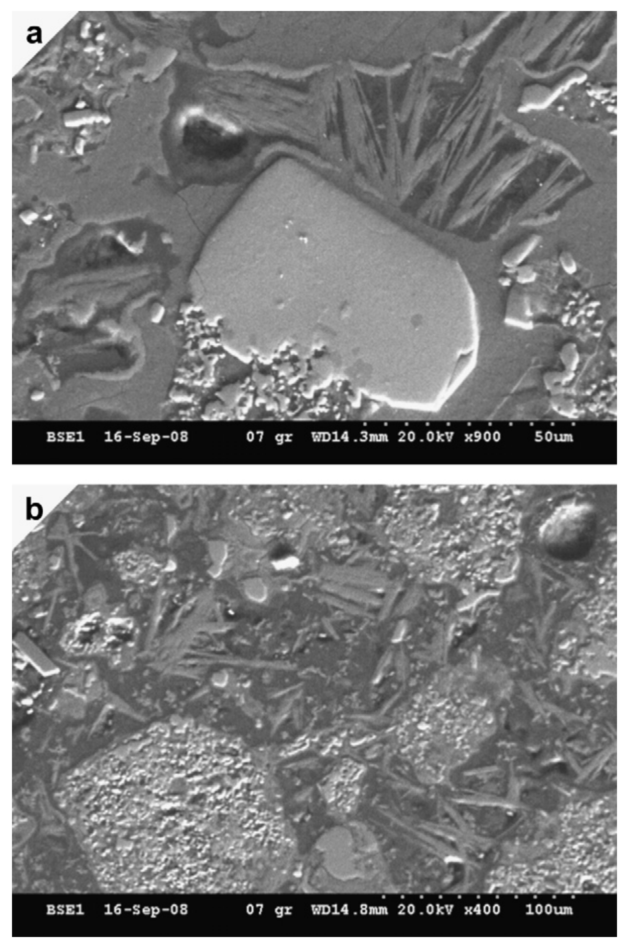

Fig. 4. Backscattered scanning electron microscope images, wall nucleus concrete, Grande Aula. a) strätlingite cement with blade-like forms fill a scoria vesicle; a cement with a blocky, equant form occurs within the scoria groundmass and shows decomposition along its lower edge; b) strätlingite cement grows among microscoriae in the cementitious matrix.

This is the blade-like pozzolanic cement (Fig. 4) that protrudes from scoriae surfaces in uneven radial spherulites and fills intergranular spaces of the cementitious matrix. In investigations of the reactions of hydrated lime ($Ca(OH)_2$) with chabazite, analcime, experimental glasses, and natural volcanic pozzolans, including Pozzolane Rosse quarried at Segni, about 50 km east of Rome, Sersale and Orsini (1969) identified strätlingite, or gehlenite hydrate, as the aluminate phase most likely to be produced at high concentrations of SiO_2 and Al_2O_3 in pore fluids of the pozzolanic mixtures. Significantly, curing of Pozzolane Rosse pozzolan-lime pastes consistently produced strätlingite and calcium alumina hydrates, indicating that precipitation of these phases is influenced by both the initial pozzolanic reaction of the ash with hydrated lime and the long term concentrations of lime in the cement environment (Sersale and Orsini, 1969). MacDowell (1991) described experimental calcium aluminate glass cements, with early-formed high compressive strengths, in which strätlingite pastes form dense continuous, bladed radial spherulite textures similar to the strätlingite in ancient wall mortars with predominantly Pozzolane Rosse ash aggregate (Fig. 4).

The modern concrete industry generally refrains from using aggregates with high alkali concentrations. Deleterious expansions produced by reaction between alkalis in the cement paste and reactive silica in the aggregates frequently lead to internal swelling, cracking, and failure in modern cements (Fournier and Bérubé, 2000). Portland cement pastes, for example, generally have Ca:Si at about 1.5 to 3 and $K_2O + Na_2O < 1$ weight percent (Van Oss, 2005:14). In comparison, the cementitious gels of Roman mortars analyzed by Roy and Langton (1989); (see also Lechtman and Hobbs, 1987) have low Ca:Si, at about 0.3 to 1.0, alumina-enriched compositions, Si:Al at about 2.5–3, and substantial alkali concentrations, with $K_2O + Na_2O$ ranging from 2.5 to 4 weight percent. Indeed, the cementitious matrix of the wall mortar of the Grande Aula has Ca:Si at about 0.6, Si:Al at 2.7, and alkali concentrations, $K_2O + Na_2O$, at 4.1 weight percent (Table 3).

Overall, these compositions suggest strong chemical interaction, or pozzolanic reactivity, between hydrated lime and Pozzolane Rosse aggregate. The alkali- and alumina-rich groundmass of silt- and sand-sized scoriae appears to be one of the predominant reactive constituents of the ash (Jackson et al., in press). Remarkably, scoriae from a least altered facies of the ignimbrite have K_2O ranging from about 3.0 to 7.5 weight percent (Table 3). Petrographic observations of thin sections of numerous mortars from the imperial age Roman monuments, however, reveal a general absence of microcracks and optical traces of alkali-silica gels (Jackson et al., in press). The alumina-rich reactive components of Pozzolane Rosse – scoria groundmass, as well as clay and zeolite surface coatings – may have increased sorption and binding of alkalis into the low Ca:Si, calcium-aluminate-silicate hydrate (Hong and Glasser, 2002) of the ancient mortars (Roy and Langton, 1989). Furthermore, desorption, or decomposition, of an alkali-rich solid phase appears to be reduced in alkali free water (Hong and Glasser, 2002). It seems that alkali sorption into the Roman low Ca:Si, high alumina, cementitious gels may have been a somewhat irreversible process, given the highly coherent microstructures of the wall mortars. Indeed, the presence of strätlingite attests to the high durability of the wall concretes and their excellent state of preservation in the Grande Aula. Notably, MacDowell (1991) describes the chemical resistance of strätlingite pastes in water and weakly acidic and basic solutions.

4. Unit weights

4.1. Wall mortars and concretes

Measurements of the bulk specific gravity (**G**) of the concrete wall nucleus of the Grande Aula, obtained from the ragged tips of the 19 cm diameter cores following the ASTM (2000) C-97-96 standards, give an average value of 1.49, indicating a unit weight of about 1490 kg/m^3 (Table 1). These values fall within the range of densities of Basilica of Maxentius (306–313 AD) concretes, which contain Pozzolane Rosse mortar aggregate (Giavarini et al., 2002, 2006). In comparison, the pozzolanic mortar of the Grande Aula concrete wall nucleus and the compositionally equivalent mortar of

Table. 3
Chemical compositions of the pozzolanic wall mortars and the vaulted ceiling mortars of the Grande Aula, and raw pumices and Pozzolane Rosse volcanic ash aggregate,-determined through x-ray fluorescence spectroscopy of fused glass beads for major element compositions.

	SiO_2	TiO_2	Al_2O_3	Fe_2O_3	MnO	MgO	CaO	Na_2O	K_2O	P_2O_5	LOI	Total	Zr	Rb	Sr	Zr/TiO_2	Rb/Sr
	weight percent oxides												(mg/kg)				
Grande Aula Concretes																	
Wall Mortar																	
07-GRAULA20a-C1	34.12	0.65	12.61	6.98	0.14	3.26	20.29	0.84	3.46	0.48	17.17	100	352	175	1038	542	0.17
07-GRAULA20a-C1*	30.65	0.59	11.08	6.75	0.13	3.93	21.7	0.78	2.51	0.47	21.42	100	339	133	1473	575	0.09
Vault mortar																	
08-GRAULA-C2	35.71	0.44	11.52	4.38	0.11	1.76	20.92	1.24	3.69	0.29	19.95	100	299	173	761	680	0.227
08-GRAULA-C2	35.92	0.46	11.51	4.67	0.12	1.91	20.58	1.17	3.52	0.3	19.94	100	327	189	894	711	0.211
08-GRAULA-C2p**	49.29	0.42	15.26	3.37	0.13	0.48	4.61	3.49	6.62	0.09	16.25	100	409	293	239	974	1.226
Roman Lime [a], limestone quarries																	
Monte Soratte	3.44	n.d.	0.3	0.31	n.d.	0.7	95.02	n.d.	n.d.	0.2	n/a	100	7	n.d.	253	n/a	n/a
Sant'Angelo Romano	3.12	n.d.	n.d.	0.19	n.d.	2.2	94.37	n.d.	n.d.	n.d.	n/a	100	4	n.d.	257	n/a	n/a
Pozzolane Rosse ignimbrite, scoriae analyses																	
06-DEO-CDL-14 [1]	46.04	1.14	21.4	10.84	0.22	1.48	1.88	0.34	2.68	0.35	13.63	100	525	177	767	461	0.23
07-CAPANN-PR-12 [2]	43.6	0.87	15.54	9.43	0.18	4.51	10.68	1.32	6.21	0.73	6.93	100	476	313	1428	547	0.22
07-STECLA-PR-3 [3]	42.9	0.9	15.09	9.41	0.16	4.3	8.31	0.6	6.95	0.74	10.64	100	513	380	1860	570	0.2
07-STECLA-PR-10 [3]	51.69	1.04	11.81	11.17	0.2	5.14	8.35	n.d.	3.27	0.26	7.07	100	509	181	960	489	0.189

* Less than one millimeter fraction
** light gray pumice aggregate
[1] Castel di Leva quarry
[2] Tenuta di Capannacce quarry
[3] Santa Tecla quarry (San Paolo Fuori le Mura) LOI records the percent by weight of volatile compounds, such as H_2O and CO_2 driven from the sample during heating above 550°C.
[a] Lime analyses reported as renormalized anhydrous weight percent
[b] n.d. = not detected (below detection limits)
[c] n/a = not analyzed

the radial pier of Bay 246 of the ground floor of the Markets of Trajan have average **G** of 1.75 (Table 2). Furthermore, five mortar specimens from the concrete walls of the Basilica Ulpia and Forum of Trajan (Bianchi et al., in press), fall in the range of 1.78 to 1.83, with average **G** = 1.79. These rather uniform specific gravity measurements and mortar aggregate compositions suggest that builders maintained consistent formulations for the wall constructions of the Markets and Forum.

4.2. Vaulted ceiling mortars

Petrographic point count analyses of thin sections of the central vaulted ceiling mortar s (Fig. 1; Table 2) indicate that it contains Pozzolane Rosse volcanic ash and, in addition, about 30–40 volume percent light gray, sanidine-bearing pumice. The XRD of the vault mortar shows leucite, diopside, and analcime associated with the Pozzolane Rosse ash aggregate and crystals of sanidine and trace amounts of diopside from the light-gray pumice aggregate (Fig. 3). Ongoing analyses will clarify the lithological provenance of the pumice in the vault mortar and the nature of its pozzolanic cements and textures.

The large vesicular voids and soft glass of the pumice create difficulties in acquiring accurate measurements of specific gravity (Wesley, 2001). The unit weight of a given volume of modern concrete equals the sum of the unit weight of its relative volume of cement paste plus the unit weights of the relative volumes of its constituent aggregates (Mindess et al., 2003, 138). To estimate the unit weights of Roman pozzolanic mortars, we sum the unit weight of each mortar constituent, multiplied by its relative proportion in the mortar determined through point counts (Table 2), using the following unit weights for mortar constituents: altered Pozzolane Rosse scoriae, 1600 kg/m^3; hydrated cementitious materials of the ancient pozzolanic cements and calcite, 2100 kg/m^3 (Mindess et al., 2003, 81); silicic pumices, 800 kg/m^3, an appropriate intermediate value based on petrographic observations; Tufo Lionato tuff particles, 1600 kg/m^3; and Tufo Giallo della Via Tiberina tuff particles, 1300 kg/m^3 (Table 1). These computations give unit weights of about 1430 to 1660 kg/m^3 for the pumice-bearing mortars from the vaulted ceiling. Similar computations for the mortars of the concrete wall cores give unit weights of about 1760–1790 kg/m^3, in good agreement with specific gravity measurements (Table 2). The pumices apparently lighten the vault mortars by about 5–20 weight percent, as compared with the average unit weight of the wall mortars. This suggests that Roman builders apparently strove to reduce the weight of the vaulted ceiling. Their selection of Tufo Giallo della Via Tiberina coarse aggregate (Lancaster, 2000) further reduced the unit weight of the vault concrete, perhaps to about 1200–1300 kg/m^3, as for the vaults of the Basilica of Maxentius (Giavarini et al., 2006).

5. Methods of tensile strength testing

The concrete walls of the Grande Aula are inherently inhomogeneous building materials, and diverse processes of fracture and failure may occur within the concrete, depending on the concrete constituents subjected to loading. The large sizes of the tuff and brick coarse aggregate relative to the 19 cm diameter, thin walled, drill cores (Fig. 1) precludes unbiased testing of the monolithic strength of the ancient concrete. We therefore designed testing experiments using a point-load device (ISRM, 1985) and small disc specimens of the concrete, to quantify the tensile strength and failure patterns of the pozzolanic mortar; the brick, Tufo Lionato tuff, and Tufo Giallo della Via Tiberina tuff clasts; and the interfacial surfaces along which these *caementa* are bonded to the pozzolanic mortar at the centimeter scale (Fig. 5).

Thirty-four tests come from 3.5 cm diameter cores that were drilled into the ragged tips of the 19 cm concrete cylinders and sliced into 1.5 cm thick discs, so that the pozzolanic mortar, the coarse aggregate clasts, or the interfacial zones would be at the centers of the specimens where the point load would be applied. Eighteen tests come from a 3.5 cm diameter core previously drilled a radial pier at Bay 246 of the Markets of Trajan, where the composition of the concrete is very similar to the Grande Aula wall nuclei (Table 2). Here, the compositions of the disc specimens reflect the random intersection of the core with the conglomeratic concrete. The fabric of most specimens varied through the 1.5 cm thickness from the top to bottom surfaces of the disc. In all instances, however, the nucleation point of rupture at the center of each disc was clearly identifiable under observation with a binocular microscope.

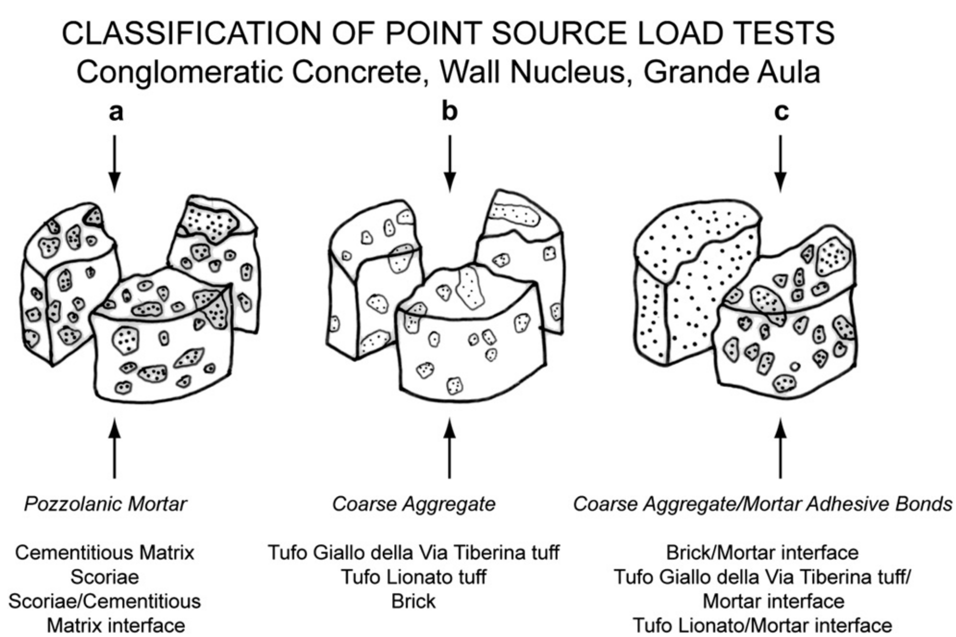

Fig. 5. Schematic diagram showing the orientation of discs with respect to the point load source and classification of disc specimen ruptures in tensile strength measurements.

Table 4
Point source tensile failure data and approximate equivalents with previous tensile strength tests. Specimens from Grande Aula core 8b, Bay 135 and core 20a, Bay 136 have average $\mathbf{f}_{pl}$ at 3.79 MPa, with high standard deviation at 2.39, indicating very heterogeneous behavior of the wall concrete at the macro-scale. Specimens from the Bay 246 radial pier at Markets of Trajan have average $\mathbf{f}_{pl}$ at 3.79 MPa, also with high standard deviation at 3.52.

Component of Conglomeratic Concrete	Point Load Test	Brazilian Test	Approximate Equivalence 1:3.25
	$\mathbf{f}_{pl}$	$\mathbf{f}_{st}$	$\mathbf{f}_{t}$
	Average tensile failure, MPa	Tensile strength, MPa	Tensile strength, MPa
Roman brick	8.7	3.33[a]	2.7
Test values – Bay 246: A3, 10.38 MPa; A4, 7.62 MPa; core 20a: A3, 9.20 MPa; A4, 8.66 MPa; A5, 11.80 MPa; J1, 7.71 MPa; J2, 7.03 MPa; J3, 6.69 MPa. Average = 8.64 MPa, *s* = 3.10			
Tufo Lionato volcanic tuff	3.6	0.8 to 1.6 [b]	1.2
Test values - Bay 246: B3, 5.07 MPa; B4, 4.64 MPa; core 20a: C4, 3.63 MPa; C5, 3.34 MPa; D3, 3.37 MPa; F1, 2.94 MPa; F2, 2.98 MPa; F3, 2.82 MPa, F4, 3.86 MPa. Average = 3.63 MPa, *s* = 0.78			
Tufo Giallo della Via Tiberina volcanic tuff	2.9	0.8 [c]	0.9
Test values - core 20a: E1, 3.22 MPa; core 8b: A1, 2.01 MPa; A2, 2.48 MPa; A3, 3.97 MPa. Average = 2.92 MPa, *s* = 0.86.			
Pozzolanic mortar, cementitious matrix	1.6 to 3.4; average ~2.5	0.95 to 1.09 [a]	0.5 to 1.6; average 0.8
Test values - cementitious matrix: Bay 246: A1, 3.21; B7, 1.56 MPa; core 20a: E3, 2.63 MPa; core 8b: C2, 2.11 MPa; J4, 3.35 MPa. Pozzolane Rosse scoriae: core 20a: A1, 3.22 MPa; A2, 4.51 MPa; core 8b: C1, 2.01. Pozzolane Rosse lava rock fragment: Bay 246: B1, 16.43 MPa. Average (without 246-B1) = 2.83 MPa, *s* = 0.94			
Roman brick - mortar interface	2.1	/	0.6
Test values - Bay 246: A2, 2.64 MPa; A5, 1.49 MPa; C5, 1.87 MPa; C6, 0.77 MPa; C7, 1.32 MPa; core 8b: B1, 1.39 MPa; B2, 1.91 MPa; B3, 3.36 MPa; G1, 4.24. Average = 1.84 MPa, *s* = 1.21			
Tufo Lionato – mortar interface	2.4	/	0.7
Test values: Bay 246: B2, 2.29 MPa; B5, 2.17 MPa; B6, 1.55 MPa; core 20a: C3, 2.01 MPa; D1, 1.45 MPa; D2, 3.66 MPa; D4, 3.45 MPa. Average = 2.37 MPa, *s* = 0.87			
Tufo Giallo della Via Tiberina - mortar interface	1.6	/	0.5
Test values - Bay 246: C2, 1.75 MPa; C3, 2.14 MPa; C4, 1.29 MPa; core 20a: C1, 1.33 MPa; C2, 1.12 MPa; E2, 1.82 MPa. Average = 1.58 MPa, *s* = 0.36			
Average (52 tests)	3.8	0.7 - 0.9 1	1.1

[a] Samuelli Ferretti, 1997.
[b] De Casa et al., 1999.
[c] Nappi et al., 1979.

Point source tests provide a reliable measure of the strength of fine-grained rocks with homogeneous textures, and have been used extensively in the evaluation of strengths of Carrara marble (Logan, 2004, 2006). Brazilian tensile tests or uniaxial tension tests (Goodman, 1989) have several disadvantages for testing of the Roman concretes. Brazilian, or splitting, tests load the test specimen along a core diameter and therefore predetermine the failure fracture orientation. As there is only a statistical probability that this is the weakest orientation, the measured strengths may be higher than those determined with the point-load technique. This does not appear to be the case for the Roman conglomeratic concretes, however (Table 4). Also, because the failure fracture orientation is predetermined in the Brazilian tests, the effects of lithologic structure or stored residual strain are frequently obscured. Furthermore, uniaxial tension specimens generally have a length to diameter ratio of at least 2:1. Given the limited amount of ancient samples available for testing, this method would greatly reduce the number of potential strength tests and present a significant obstacle in understanding the mechanical and fracture behavior of the conglomeratic concretes.

Prior to testing, we made precise measurements of the diameter and thickness of each disc specimen. We oven-dried the test specimens at 95 °C for 24 h and placed them in a vacuum chamber until tested. To measure the strength, we placed the test disc in a specimen holder that has two small, embedded ball bearings centered on the opposite flat surfaces. We centered the test specimen in the specimen holder and stroked a hydraulic pump at a constant rate to load the specimen to failure; that is, rupture into a complete separation of parts. We monitored a pressure gauge during the loading to ensure constant loading rates and record any premature force drops that might occur before ultimate tensile failure. A marking needle remained steady at this failure pressure after the load dropped. We then recorded the failure pressure and converted it to a value of tensile strength. Strains were not measured. Failure of specimens with high strength, above about 6 MPa, was accompanied by a single, loud, acoustic emission. In specimens of low strength, very soft acoustic clustered emissions were sometimes heard; these sounded as if they were distributed through the specimen. In some stronger specimens, a few soft, single sounds occurred before the loud emission accompanying total specimen failure. After removing the specimen from the test holder and taping it back together, we mapped the induced macro- and micro-fractures on page-sized scans of each surface of the ruptured disc with a stereomicroscope.

The character, orientation, and length scale of the concrete failure are described using the following terminology: *rupture* refers to the centimeter-sized break or breach directly induced by the point load test, which usually leaves a gap, rift, or fissure in the concrete fabric; *fracture* refers to a break or fissure in the concrete fabric at the meter-scale, or the structural and architectural scale; *macrofracture* refers to a break or fissure at the centimeter-scale that is visible at the level of the hand sample or macrostructure of the concrete fabric; *microfracture* refers to a break at the cementitious matrix or micro-meter scale; and *microcrack* refers to a flaw or defect in the concrete fabric that may, when subjected to loads, coalesce or bridge together with other microcracks to form microfractures or macrofractures.

6. Results of point load testing experiments

The concrete disc specimens from the Grande Aula wall concrete record a wide range of ultimate tensile failure ($\mathbf{f}_{pl}$), from 11.8 MPa to 1.12 MPa, with an average strength of 3.79 MPa and a large standard deviation at 2.39 MPa (Fig. 6). Testing of 18 specimens from the radial pier on the first floor of the Markets of Trajan at Bay 246 yields average tensile failure identical to the Grande Aula tests, 3.79 MPa, also with a high standard deviation (Fig. 6).

Mapping of disc surfaces, however, reveals that 21 specimens record tensile failure of coarse aggregate clasts: brick, average $\mathbf{f}_{pl}$ at 8.7 MPa; Tufo Lionato tuff, average $\mathbf{f}_{pl}$ at 3.6 MPa; and Tufo Giallo

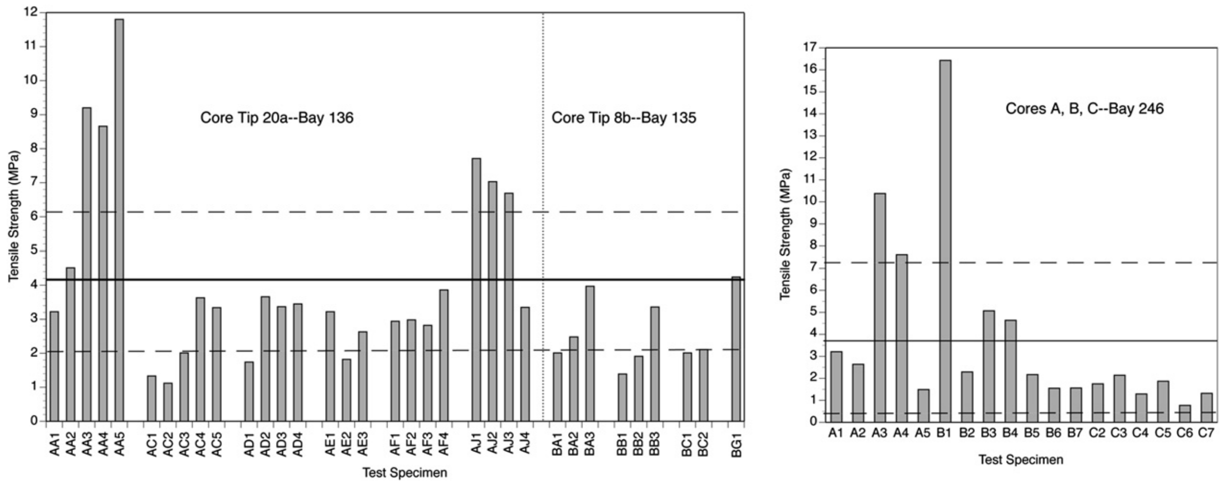

Fig. 6. Histograms showing the ultimate tensile failure strengths of disc specimens recorded by point load testing experiments on the conglomeratic wall concretes.

della Via Tiberina tuff, $\mathbf{f}_{pl}$ at 2.9 MPa (Table 4). In many tests the initial macrofracture propagated to the boundary of the aggregate clast, and then produced a new macrofracture with an entirely different orientation, commonly along the edge of the clast. Twenty-two specimens recorded rupture at the interface of coarse aggregate clasts with the pozzolanic mortar: brick–mortar interfaces have average $\mathbf{f}_{pl}$ at 2.1 MPa; Tufo Lionato tuff–mortar interfaces have average $\mathbf{f}_{pl}$ at 2.4 MPa; Tufo Giallo della Via Tiberina tuff–mortar interfaces have $\mathbf{f}_{pl}$ at 1.6 MPa. The standard deviations for each of these seven groups of tests is significantly less than the overall standard deviation for the 52 tests (Table 4), except for the brick clasts which have a wide range of strengths, as noted by Samuelli Ferretti (1997). The brick–mortar interfaces also showed a large dispersion of strengths, 0.77 MPa to 4.24 MPa. This may result from

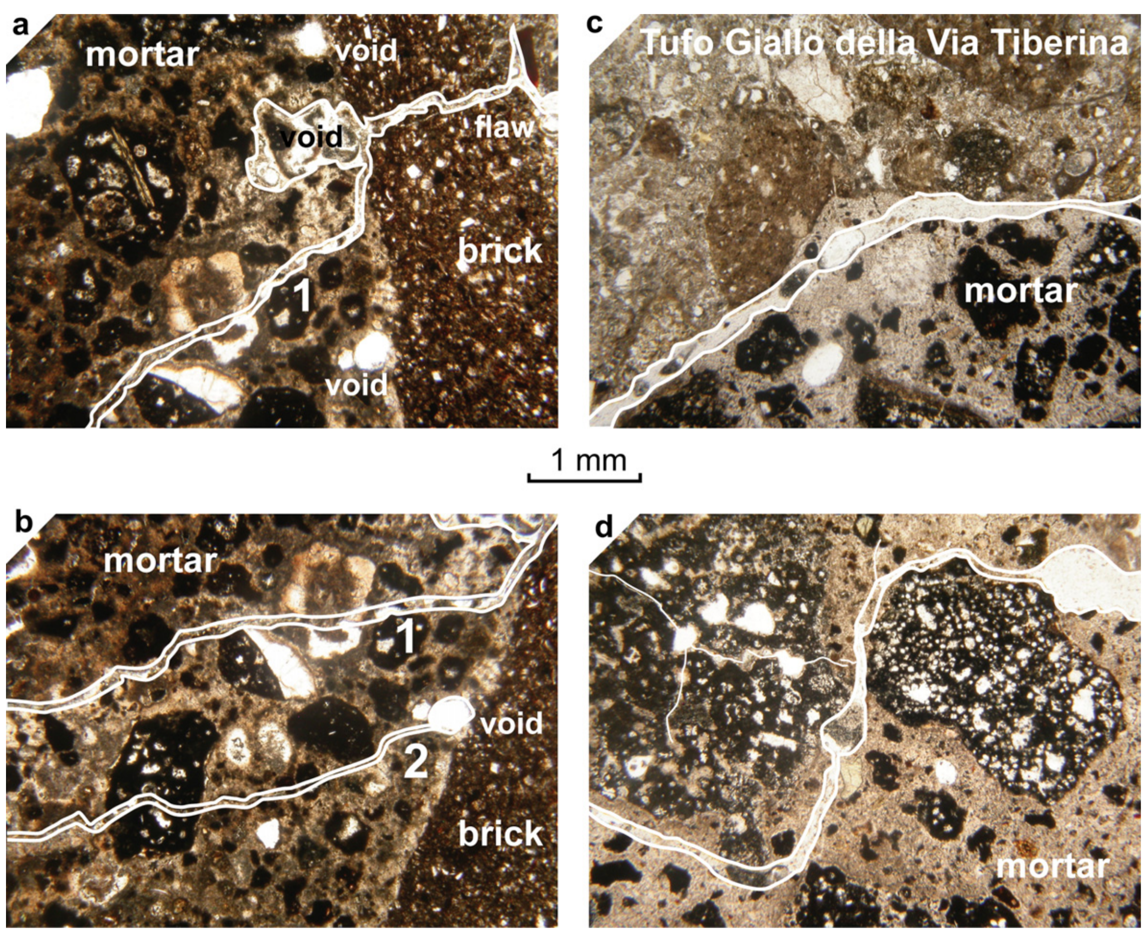

Fig. 7. Photomicrographs showing microcracks induced by point loads tests in disc specimens of wall nucleus concrete. a, b) rupture at $\mathbf{f}_t = 0.8$ MPa of disc specimen Bay 246:A2 nucleated at a flaw at the edge of brick coarse aggregate, and continued into the pozzolanic mortar, producing somewhat smooth microcracks that split Pozzolane Rosse scoriae; c, d) rupture at $\mathbf{f}_t = 0.4$ MPa of disc specimen Bay 234:C4 nucleated along the Tufo Giallo della Via Tiberina tuff – pozzolanic mortar interface, and continued into the pozzolanic mortar, producing a curving microcrack with high surface roughness that winds among Pozzolane Rosse scoriae.

1) pervasive millimeter-sized, open voids along brick–mortar contacts that appear to substantially reduce interfacial adhesion (Figs. 2 and 7a, b; Table 4, specimen Bay 246-C6), 2) possible localized strengthening of the interfacial contacts in areas where brick fragments form a clast-supported framework in the concrete (Fig. 2, lower left quadrant; Table 4, specimen Core 8b-G1), and/or 3) the wide range of brick mechanical properties noted by Samuelli Ferretti (1997) that may encourage microfracture and macrofracture at microcracks along clast perimeters.

Finally, nine disc specimens recorded failure of components of the pozzolanic mortar. Gravel-sized Pozzolane Rosse scoriae record point load tensile failure, $\mathbf{f}_{pl}$, from 2.0 MPa to 4.5 MPa. (A coarse gravel-sized Pozzolane Rosse lava rock fragment records $\mathbf{f}_{pl}$ at 16.4 MPa.) The cementitious matrix of the mortar records $\mathbf{f}_{pl}$ at 1.6 MPa to 3.5 MPa, and the nucleation of ruptures in two specimens at the interface of Pozzolane Rosse scoria with the cementitious matrix record tensile strengths that fall within this range. The average $\mathbf{f}_{pl}$ of the cementitious matrix of the mortar could be about 2.5 MPa, based on the limited testing data. The test results suggest that the cementitious matrix may have a lower tensile strength than that of the overall concrete, which has average $\mathbf{f}_{pl}$ at about 3.8 MPa (Table 4).

6.1. Influence of compositional variations

The interfacial bonds that join the Tufo Giallo della Via Tiberina tuff clasts to the mortar seem to be the most vulnerable connection in the conglomeratic concrete fabric.

The tuff contains pumice fragments that have glass altered to clay mineral (Nappi et al., 1979; Jackson et al., 2005). The porous, friable texture of these altered pumices, which readily disintegrate into fine, opaque powder, may reduce the adherence of pozzolanic cements. Furthermore, experimental studies of the accelerated alteration of tuff bearing concretes in circulating groundwater indicate that the chemical reactivity of the vitreous components of the tuff may produce microcracking at interfaces with the cementitious matrix and unpredictable changes in the mechanical properties of the concrete (Scheetz and Roy, 1969).

Overall, the edges of *caementa* clasts appear to be the surfaces of greatest weakness within the wall nuclei concretes. Fig. 6a shows a rupture that apparently initiated at the intersection of a preexisting flaw at the edge of the brick clast and a tiny void in the brick–mortar interfacial zone. These millimeter-sized gaps in the surface bond are common along the edges of the brick. A microfracture (location 1, Fig. 7b) apparently formed perpendicular to the brick–mortar contact and continued into the cementitious matrix for several centimeters. Another microfracture propagated from a void at the edge of the brick (location 2, Fig. 7b), producing opening displacements through several fine sand-sized Pozzolane Rosse scoriae (Fig. 7b). The microfractures form a fracture process zone, or damage zone, about 1 to 2 mm wide, which appears to coalesce downwards, forming a through going macrofracture with opening displacement on the lower disc surface.

In contrast, a rupture at a Tufo Giallo della Via Tiberina tuff–pozzolanic mortar interface (Fig. 7c) apparently produced a microfracture that continued along the edge of the tuff clast into the cementitious matrix of the pozzolanic mortar. It then wound between Pozzolane Rosse scoriae (Fig. 7d), producing a microfracture with high surface roughness, and series of microfracture segments that continued through the cementitious matrix. Overall, the microfractures form a 1 to 2 mm thick fracture process zone that apparently propagated upwards, producing a through going macrofracture with opening displacement on the upper disc surface. The variations in micro- and macro-fracture structures may be the result of varying magnitudes of local tensile stress levels and inelastic deformation, which may have developed as a function of the relative strength of the aggregate or the aggregate/mortar interfaces and varying heights in a fracture process zone, adjacent to the main opening rupture (Pollard and Fletcher, 2006: 354).

The relatively low tensile strengths of the mortar and its somewhat tenuous adhesion to coarse aggregate clasts in interfacial zones suggests that the *caementa* may have had a significant role in arresting the propagation of tensile microcracks that formed in the mortar, thereby increasing the composite tensile strength of the concrete. This is potentially quite important to understanding the overall strength of ancient concrete masonry structures, but it needs to be evaluated on tests of larger samples, where complete interfacial zones are present.

6.2. Comparison of point-load tensile strengths with other strength measurements

Attempts to correlate point load measurements of tensile strength with Brazilian test results have been made on other rock types, such as Carrara marble, that are far more homogeneous with respect to composition and grain size than the ancient concretes (Logan, 2004, 2006). Although Brazilian tests have disadvantages for evaluating the strengths of the Roman conglomeratic concretes, as discussed above, they provide a *de facto* standard measure of tensile strengths ($\mathbf{f}_{st}$) (Elices and Planas, 1996). We have therefore attempted to correlate the point load test results with the sparse Brazilian tensile strength data available for the Roman concretes and their constituent aggregates. There is fairly regular, average correlation of about 1:3.25 between splitting test values ($\mathbf{f}_{st}$) and the point load values ($\mathbf{f}_{pl}$) of the individual types of *caementa* and the ancient and experimental pozzolanic mortars (Tables 1 and 4). This tentative, approximate correspondence suggests averaged tensile strengths ($\mathbf{f}_t$) of about 2.7 MPa for brick, 1.1 MPa for Tufo Lionato tuff, 0.9 MPa for Tufo Giallo della Via Tiberina, and 0.75 MPa to 1.6 MPa for pozzolanic mortar (Table 4, Fig. 8). Uncertainties remain in identifying a similar correspondence for mortar–*caementa* interfacial zones, because no previous experimental data exists for these elements of the concrete fabric. Even so, using the

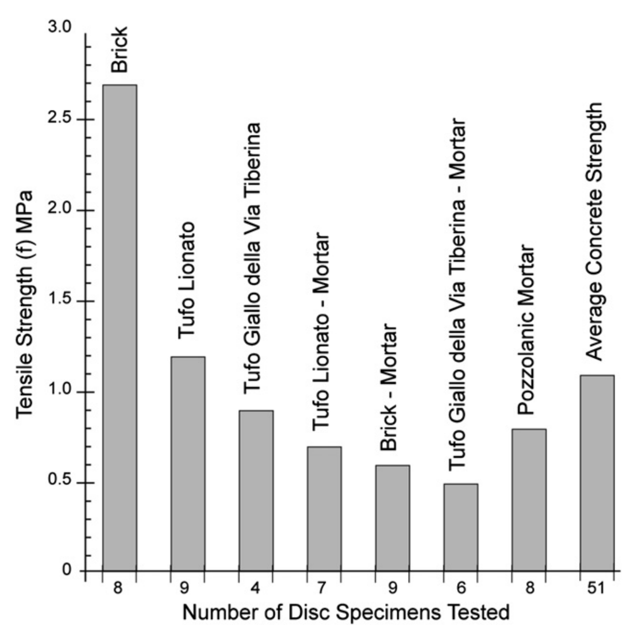

Fig. 8. Tensile strengths of components of the wall concretes from point source tests, grouped by the lithological compositions of coarse aggregate (*caementa*) and structural role in the conglomeratic concrete fabric (The tensile strength, $\mathbf{f}_t$, at 5.05 MPa of the Pozzolane Rosse lava lithic fragment, disc specimen Bay 246:B1, is not included.).

same 1:3.25 equivalence suggests that adhesive tensile strengths ($\mathbf{f}_t$) could be as low as about 0.7 MPa for the Tufo Lionato tuff–mortar interface, 0.6 MPa for the brick–mortar interface, and 0.5 MPa for the Tufo Giallo della Via Tiberina tuff–mortar interface (Table 4; Fig. 7). These interfacial contact zones, which appear to be the weakest connections in the ancient concrete fabric, appear to have tensile strengths that may be about 1/10 of the average compressive strength measured for the ancient concretes, about 6 MPa (Table 1) (Giavarini et al., 2006). In particular, the splitting tensile strength ($\mathbf{f}_{st}$) of concrete cores with brick aggregate from the Villa Adriana (AD 145) is 0.7 to 0.9 MPa, about 0.13 of the compressive strength. In modern concretes the ratio of splitting tensile strength to compressive strength generally ranges from 0.08 to 0.14 (Mindess et al., 2003: 315).

A size effect influences testing results of modern concretes, such that tests on smaller samples generally produce higher compressive and tensile strengths than tests on larger samples (Carpinteri et al., 2004). The tentative 1:3.25 correspondence between larger Brazilian splitting tests ($\mathbf{f}_{st}$) (Table 4) and the smaller point source tests ($\mathbf{f}_{pl}$) of the ancient wall concretes may follow this effect. Larger specimens with larger aggregates may produce longer coalescing macrocracks that link to form longer macrofractures with greater displacements, which hasten ultimate tensile failure. Further experimental tests, structural mapping, and mechanical modeling of the ancient concretes will clarify the nature of this size effect at the structural scale of the Grande Aula.

7. Composite strengths of the conglomeratic concretes

Failure by adhesion rupture between the *caementa* and the cementitious matrix of the pozzolanic mortar appears to vary among the different types of coarse aggregate clasts (Fig. 7; Table 4). The average tensile strength of Tufo Giallo dell Via Tiberina tuff seems to be quite close to the adhesive strength of its interface with the pozzolanic mortar, and induced microfractures along the tuff–mortar interface commonly propagate into the host tuff clast, producing a complex pattern of macrofracture. In contrast, the average tensile strength of the brick clasts seems to be two or three times higher than the brick-mortar interface and the cementitious matrix (Tables 1 and 4; Fig. 8). Microfractures seem to nucleate at microcracks, mainly millimeter-sized voids along rectilinear surfaces of the brick–mortar interface. These apparently coalesce to form macrofractures that tend to continue into the mortar, leaving the brick largely intact. Builders clearly endeavored to vigorously compact the wet concrete mass, as illustrated by the tight mortar joints of the wall concrete (Fig. 2), but they seem not to have been able to avoid these vesicular flaws against the smooth margins of the brick. Although the average tensile strength of the Tufo Lionato tuff is generally less than that of the brick, the rough surfaces of the glassy, zeolitic tuff clasts (Jackson et al., 2005) may enhance mechanical and pozzolanic adhesion with the mortar.

Paradoxically, the strongly heterogeneous nature of the strength and deformability of the various elements of the conglomeratic fabric of the wall nucleus concrete may be a key factor in the durability of the wall masonry. Acoustic emissions recorded during the point source tests suggest that microfractures may initiate at low applied loads and continue through the deformation process until ultimate failure. Finite Element modeling to determine stress distributions and magnitudes under gravitational loading within the Grande Aula (Perucchio and Brune, in press), suggests that significant tensile stresses may develop along interior cross-sections within the concrete lateral arches and vault supports, which appear to have compositions similar to the wall nuclei. On exterior sections, numerical computations predict that tensile stresses in the range of 500 KPa may develop along the interior vault supports (Perucchio and Brune, in press). These concretes contain pervasive macrofractures, but further observations are needed to clarify the type(s) of coarse aggregate and fracture patterns. Furthermore, the central vault of the Grande Aula displays pervasive fractures yet remains fundamentally intact (Ungaro and Vitti, 2007). Mapping of such structures, using photographs to construct maps similar to Fig. 2, will provide insights into the strengths and stabilities of the concretes as a function of their composition and structural position.

Roman builders apparently formulated the mortars of the vaulted ceiling of the Grande Aula with about 30 to 40 percent by volume pumices to introduce voids into the concrete and lessen its unit weight (Table 2). Intriguingly, however, the pumiceous clasts could have stronger interfacial adhesive bonds and higher tensile strength than the Pozzolane Rosse scoria-mortar bonds (Gündüz and Ugur, 2005), thus adding greater durability to the vaulted ceiling. Future point load tests of drill cores of vault concrete from the Markets of Trajan should help clarify these relationships.

8. Conclusions

Compositional analyses and tensile strength testing results confirm that processes of fracture and failure at the macro-scale depend on which components of ancient conglomeratic concretes are subjected to loading. Based on point source load tests of the wall nucleus concretes and a tentative correspondence with splitting tensile tests, the tensile strengths ($\mathbf{f}_t$) of the brick, Tufo Lionato tuff, and Tufo Giallo della Via Tiberina tuff coarse aggregate clasts, about 2.7 MPa, 1.1 MPa, and 0.9 MPa, appear to be consistently higher than tensile strengths of their bonds with the pozzolanic mortar, about 0.7 MPa, 0.6 MPa, and 0.5 MPa (Fig. 7). Significantly, the heterogeneous strengths of the coarse aggregate components of the conglomeratic concrete fabric may be a determining factor in maintaining the composite cohesive strength of the concrete masonry at the structural scale. The strätlinglite and calcium–alumina–silica pozzolanic cementitious phases of the wall nucleus mortars appear to be a key factor in enhancing the long-term durability of the concretes. Indeed, the presence of strätlingite in the wall mortars attests to their high durability and the excellent state of preservation of the Grande Aula.

Overall, the complexity of the aggregate mixtures that Roman builders selected for both the pozzolanic mortars and the conglomeratic concrete *caementa*, the attention that they gave to closely compacting the wet concrete mass, the forethought that they obviously paid to developing differential unit weights in the concrete formulations, and the empirical knowledge of material strengths that they clearly brought to designing the diverse wall nucleus and vault concretes, bears testament to their extraordinary empirical understanding of the material characteristics of pozzolanic cements and conglomeratic concretes.

Acknowledgements

We would like to express our appreciation to C. Piastrini, N. Wonderling, T. Hoisch, and the Istituto Nazionale di Vulcanologia e Geofisica in Rome for research support. The paper benefitted from insightful discussions and review by P. Brune.

References

ASTM, 2000. Absorption and bulk specific gravity of dimension stone (C 97-96). In: Annual Book of ASTM Standards, Dimension Stone. American Society for Testing and Materials, Philadelphia 4, 04.07, 1–3.

Bianchi, E., Meneghini, R., Jackson, M., Brune, P., Marra, F., in press. Archaeological, structural, and compositional observations of the concrete architecture of the Basilica Ulpia and Trajan's Forum. Acta Instituti Romani Finlandiae.

Bianchini, M., 1991. I Mercati di Traiano. Bolletino di Archaeologia del Ministero dei Beni Culturale e Ambientali 8, 102–121.
Brune, P., Perucchio, R., in press. Numerical simulation of the mechanical behavior of Opus Caementicium: Opportunities and challenges. Acta Instituti Romani Finlandiae.
Carpinteri, A., Cornetti, P., Puzzi, S., 2004. A stereological approach of aggregate scaling and size effect on concrete tensile strength. International Journal of Fracture 128, 233–242.
Croci, G., 1993. Structural history of the Colosseum, Rome. Structural Engineering International 3, 14–16.
De Casa, G., Lombardi, G., Meucci, C., Galloni, R., Vitali, P., 1999. Il Tufo Lionato dei monumenti Romani: Caratteri petrografici, geomeccanici, e trattamenti conservati. Geologica Romana 35, 1–25.
Eichholz, D.E., 1962. Pliny, Natural History, Books 36–37 (translator). Harvard University Press, Cambridge (reprint 2001).
Elices, M., Planas, J., 1996. Fracture mechanics parameters of concretes: an overview. Advances in Cement Based Materials 4, 116–127.
Fournier, B., Bérubé, M.A., 2000. Alkali-aggregate reaction in concrete: a review of basic concepts and engineering applications. Canadian Journal of Civil Engineering 27, 167–191.
Giavarini, C., Santarelli, M.L., Torracca, G., 2002. Basilica di Massenzio: Studi dei materiali e dei fenomeni di degrado delle strutture murarie. Ministero per i Bene e le Attività Culturali Cistec report SAR 107, Soprintendenza Archeologica di Roma, Rome.
Giavarini, C., Samuelli Ferretti, A., Santarelli, M.L., 2006. Mechanical characteristics of Roman opus caementicium. In: Kourkolis, S.K. (Ed.), Fracture and Failure of Natural Building Stones. Springer, Dordrecht, pp. 107–120.
Giovannoni, G., 1913, Prototipi di archi rampanti in costruzioni romane. Annali della Societa Ingegneria ed Architettura Italiana 10.
Goldsworthy, H., Min, Z., 2009. Mortar studies towards the replication of Roman concrete. Archaeometry 51.
Goodman, R.E., 1989. Rock Mechanics. John Wiley and Sons, New York.
Granger, F., 1931. Vitruvius On Architecture, Books I–IV (translator). Harvard University Press, Cambridge (reprint 2002).
Gündüz, L., Ugur, I., 2005. The effects of different fine and coarse pumice aggregate/cement ratios on the structural concrete properties without using any admixtures. Cement and Concrete Research 35, 1859–1864.
Hong, S.Y., Glasser, F.P., 2002. Alkali sorption by C–S–H and C–A–S–H gels, Part II. Role of Alumina. Cement and Concrete Research 32, 1101–1111.
ISRM, 1985. Suggested method for determining point load strength. International Journal of Rock Mechanics Mineral Science Geomechanical Abstracts 22, 53–60.
Jackson, M.D., Marra, F., Hay, R., Cawood, C., Winkler, E., 2005. The judicious selection and preservation of tuff and travertine building stone in ancient Rome. Archaeometry 47, 485–510.
Jackson, M., Marra, F., 2006. Roman stone masonry: volcanic foundations of the ancient city. American Journal of Archaeology 110, 403–446.
Jackson, M., Marra, F., Deocampo, D., Vella, A., Kosso, C., Hay, R., 2007. Geological observations of excavated sand (harenae fossiciae) used as fine aggregate in Roman pozzolanic mortars. Journal of Roman Archaeology 20, 25–52.
Jackson, M., Deocampo, D., Marra, F., Scheetz, B., in press. Mid-Pleistocene Pozzolanic Volcanic Ash in Ancient Roman Concretes. Geoarchaeology.
Karner, D.B., Marra, F., 1998. Correlation of fluviodeltaic aggradational sections with glacial climate history: a revision of the classical Pleistocene stratigraphy of Rome. Geological Society of America Bulletin 110, 748–758.
Karner, D.B., Marra, F., Renne, P.R., 2001. The history of the Monti Sabatini and Alban Hills volcanoes: groundwork for assessing volcanic–tectonic hazards for Rome. Journal of Volcanology and Geothermal Research 107, 185–219.
Langton, C., Roy, D., 1984. Longevity of borehole and shaft sealing materials: characterization of ancient cement based building materials. Material Research Society Symposium Proceedings 26, 543–549.
Lancaster, L., 2000. Building Trajan's Markets 2: the construction process. American Journal of Archaeology 104, 755–785.
Lechtman, H.N., Hobbs, H.W., 1987. Roman concrete and the Roman architectural revolution. Ceramics and Civilization 3, 81–128.
Logan, J.M., 2004. Laboratory and case studies of thermal cycling and stored strain on the stability of selected marbles. Environmental Geology 46, 456–467.
Logan, J.M., 2006. On-site and laboratory studies of strength loss in marble on building exteriors. In: Kourkolis, S.K. (Ed.), Fracture and Failure of Natural Building Stones. Springer, Dordrecht, pp. 345–362.
MacDowell, J.F., 1991. Strätlingite and hydrogarnet from calcium aluminosilicate glass cements. In: Scheetz, B.E., Landers, A.G., Odler, I., Jennings, H. (Eds.), Specialty Cements with Advanced Properties. Material Research Society Symposia Proceedings 179, pp. 159–179.
Marra, F., Karner, D.B., Freda, C., Gaeta, M., Renne, P.R., 2009. Large mafic eruptions at the Alban Hills Volcanic District (Central Italy): chronostratigraphy, petrography and eruptive behavior. Journal of Volcanological and Geothermal Research, 217–232.
Massazza, F., 1998. Pozzolana and pozzolanic cements. In: Lea's Chemistry of Cement and Concrete, fourth ed. Arnold Publishers, London, pp. 471–632.
Mindess, S., Young, J.F., Darwin, D., 2003. Concrete. Pearson Education, Inc., Upper Saddle River.
Nappi, G., De Casa, G., Volponi, G., 1979. Geologica e caratteristiche tecniche del "Tufo Giallo della Via Tiberina". Bulletino Societa Geologica Italiana 98, 431–445.
Oleson, J.P., Brandon, C., Cramer, S.M., Cucitore, R., Gotti, E., Hohlfelder, R.L., 2006. Reproducing a Roman maritime structure with Vitruvian pozzolanic concrete. Journal of Roman Archaeology 19, 29–52.
Perucchio, R., Brune, P., in press, Non-functional contrasting arches as revealed by the structural analyses of the Grande Aula of Trajan's Markets. In: Ungaro, L. and Vitti, M. (Eds.), La Grande Aula dei Mercati di Traiano Restituita, Bulletino della Commissione Archeologica Communale di Roma.
Penta, F., 1956. Materiali Naturali da Construzione del Lazio. Arti Grafiche Panetto e Petrelli, Rome.
Pollard, D.D., Fletcher, R., 2006. Fundamentals of Structural Geology. Cambridge University Press, Cambridge.
Roy, D.M., Langton, C.A., 1989. Studies of ancient concrete as analogs of cementitious sealing materials for a repository in tuff. Report LA-11527-MS, UC-721, prepared by the Materials Research Laboratory, Pennsylvania State University, for Los Alamos National Laboratory. Los Alamos, New Mexico.
Samuelli Ferretti, A., 1997. Proposte per lo studio teorico-sperimentale della statica dei monumenti in opus caementicium. Materiali e Strutture 7, 63–83.
Samuelli Ferretti, A., 2005. The structures of the Basilica. In: Giavarini, C. (Ed.), The Basilica of Maxentius, the Monument, its Materials, Construction, and Stability. L'Erma di Bretschneider, Rome, pp. 161–257.
Scheetz, B., Roy, D., 1969. Reactivity of tuff-bearing concrete. CL-40 CON-14. Report LA-11532-MS, UC-721, prepared by the Materials Research Laboratory, Pennsylvania State University, for Los Alamos National Laboratory. Los Alamos, New Mexico.
Sersale, R., Orsini, P.G., 1969. Hydrated phases after reaction of lime with 'pozzolanic' materials or with blastfurnace slags in: Proceedings, Fifth International Symposium on the Chemistry of Cement. pp. 114–121.
Taylor, H.F.W., 2004. Cement Chemistry. Thomas Telford, London.
Trigila, R., Agosta, E., Currado, C., De Benedetti, A., Freda, C., Gaeta, M., Palladino, D.M., 1995. Petrology. In: Trigila, R. (Ed.), The Volcano of the Alban Hills. Tipografia S.G.S., Rome, pp. 33–71.
Ungaro, L., Vitti, M., 2007. I Mercati di Traiano affrontano il nuovo millenio. Forma Urbis XII.2, 4–15.
Van Oss, 2005. Background facts and issues concerning cement and cement data, U. S. Geological Survey Open File Report 2005–1152.
Ventriglia, U., 1971. La Geologia nella città di Roma. Amministrazione Provinciale di Roma, Rome.
Vitti, M., 2007. Mercati di Traiano. In: Ungaro, L. (Ed.), Il Museo dei Fori Imperiali nei Mercati di Traiano. Electra, Milano, pp. 5–19.
Vola, G., Gotti, E., in press. Mineralogical and petrographic characterization of ancient Roman hydraulic concrete cores from Santa Liberata, Grossetto, Italy, and Caesarea Palestrinae, Israel. Acta Instituti Romani Finlandiae.
Wesley, L.D., 2001. Determination of specific gravity and void ratio. American Society for Testing of Material Geotechnical Testing Journal 24, 418–422.